https://doi.org/10.48048/tis.2022.5746

Analytical Study of Rectangular Concrete-Filled Tubes (RCFT) Connections using Finite Element Analysis under Cyclic Loading

Cintantya Budi Casita[1], Budi Suswanto[2] and Indra Komara[2,3,*]

[1]Department of Civil Engineering, Faculty of Engineering, University of Pembangunan Nasional Veteran East Java, Surabaya 60294, Indonesia
[2]Department of Civil Engineering, Faculty of Civil, Planning and Geo-Engineering, Institut Teknologi Sepuluh Nopember, Surabaya 60117, Indonesia
[3]Department of Civil Infrastructure Engineering, Faculty of Vocation, Institut Teknologi Sepuluh Nopember, Surabaya 60116, Indonesia

([*]Corresponding author's e-mail: indra@its.ac.id)

Received: 28 May 2021, Revised: 6 July 2021, Accepted: 13 July 2021

Abstract

Recent condition of the earthquakes model has shown that rectangular concrete-filled tubes (RCFT) with weld connection are so brittle. According to the studies conducted, large damages are due to the cracking of the weld between the beam flange and the column face and inducing concentrated stresses in this area. One of the novel alternatives to reduce the stress concentration at the panel zone could be the use of the reduce beam section (RBS). Given the enormous impact of seismic behaviour and ductility of the panel zone, RBS moves plastic hinges formation at an appropriate distance from column face. In this study, 2 major model of RCFT with and without RBS have been modeled using ABAQUS computer program and compared under cyclic behaviour. The obtained result of this study showed that using RBS is more ductile and implied a good stability. It also will consider having better ductility than other connections.

Keywords: Concrete-filled tubes, Reduced beam section, Connection, Cyclic load, Ductility

Introduction

Rectangular concrete-filled tubes (RCFT) beam-column are generally implied in a building construction, as they merge the potentials of compressive strength concrete capacity and well-performed ductility [1]. In a RCFT structure, the concrete and steel jointly connect one and another, in detail, the steel sheet avoids the concrete from delaminating or spalling, and the concrete inside avoids the steel from buckling [2]. The steel as the outer functionally works as a confinement, the concrete inside the steel, significantly increased the compressive strength [3]. In the other hand, the concrete inside the steel can also raise the flexural capacity and torsional capacity [3,4]. Due to its benefits and less cost in the construction, it makes RCFT commercially attractive than other preferences [5]. RCFT columns for the example are increasingly used in variety construction and infrastructure, which are presents as buildings, bridges, towers and etcetera.

Another consideration for using RCFT is avoiding to have a very large dimension in the structure. It can increase the capacity and its behaviour more likely can withstand larger flexural condition within a larger rigidity point even it uses a smaller dimension. The sectional dimension of column structure for example mainly subjected to the axial loads, as the deduction the compressive strength coming from concrete can be used, this structure are so RCFT built-up columns are comprehensively used in structural members with higher stories within higher load eccentricity and slenderness ratio, such as factory, ballroom and stadium [6]. Another implementation of RCFT used for the pillar nearly to the abutment or arch bridge with the position of continued deck. This method will reduce the total self-weight of the structure and decrease the deformation. Reasonably, the whole capacity of the bridge will be improved especially in the structural rigidity and the stress distribution, advancing the competitiveness of bridge with a larger span [7]. However, it needs specific configuration of the connection to provide a prominent behaviour under building or bridge structure.

In the concentration of beam-column joint, the region is measured by the lower and the upper beam flanges which is also can be called as the panel zone (PZ) [8]. The PZ is regularly strengthened to counter bending outward of the column flange by added steel plate, when the beam is exposed to tensile force. The common member element for strengthening the PZ consist of external diaphragms and internal diaphragms which is informed in the **Figure 1**. External diaphragms are steel plate inherent horizontally to the beam flanges, surrounding the steel column [9] at the same condition, internal diaphragms are steel plate that horizontally adjusting to the heights of the beam flanges [2]. Typically, this join has 2 internal diaphragms or 2 external diaphragms. The shapes of steel core and diagram plates can possibly be different such as, circular, square or rectangular.

In comprehensive way to fully understand the behaviour which not limited to mechanical performance of the connection, experimental program is conducted on the specimens of beam-column joint with 2 variable setups at the supports, e.g., a given loading at the ends column with fixed beam ends or given oppositely [10-12]. Nevertheless, the beam-column joint is loaded to bending moment and shear force. To achieve a high-rotational stiffness, the local relative rotation between the beam-column should be limited. Such condition can be measured by 2 inclinometers [13], in detail, the position placed on the PZ and the other position placed at the beam end. The different of those 2 measuring results is the used of inclinometers that handle the angle of the rotation of the joint. This measuring can also be evaluated by potentiometers or linear variable differential transformers which is installed between the column and the beam end [7,14,15].

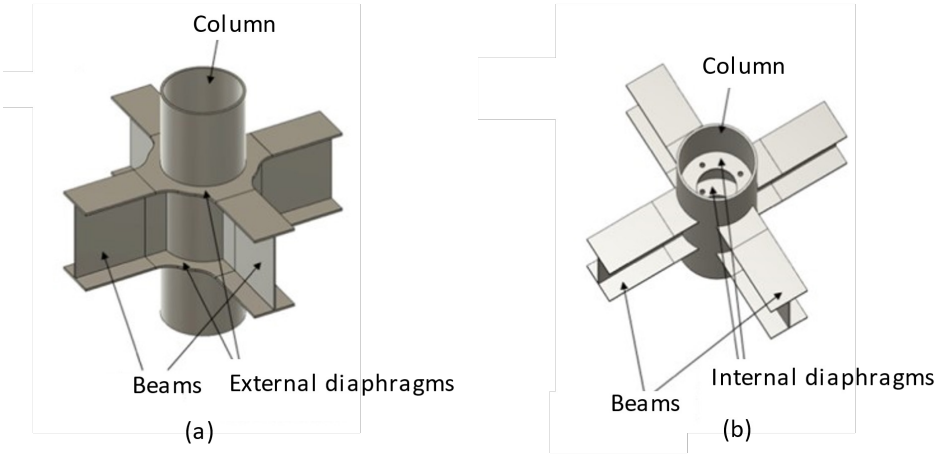

Figure 1 RCFT connection to beam-column joint; (a) external diaphragms, (b) internal diaphragms [16].

Previous study was conducting various experimental investigation performing the physical and mechanical performances of beam with concrete filled tube (CFT) column connections. As the example, end-plate connection between steel beams and CFT column without PZ stiffening were investigated experimentally where the semi-rigid and partial strength were also measured [17]. Another investigation was presented by [2], compare the steel beam to CFT column connections with and without external diaphragms. The result showed that the external diagrams in the connection offered in about 20 % higher potential of moment-rotation stiffness and moment capacity than the connection of the same sizes without diaphragms [18]. This is also assumed that this connections type can possibly provide satisfactory moment capacity which affect beam tend to fail prior to the joint. In addition, both type of connections, using internal and external diaphragms not only offer high rotational stiffness but also offer as a rigid connection [19]. In fact, this connection with internal diaphragms or external diaphragms are both advisable for 2-way frames, which can carry lateral loads from 2 horizontal directions [20]. The CFT can also be considered to be filled with cementitious materials or paste concrete such as engineered cementitious composite [21-27].

The connection of CFT have been conducted by previous research studied over the past several decades. For example: Xu *et al*. (2015) in [28] investigated 4 types (T, Y, K and, KT) of concrete-filled tubular circular hollow section (CHS) connections, Chiew *et al*. (2001) in [29] investigated 8 specimens of concrete-filled tube (CFT) connections with different types of stiffening details, which half of those number of connections were semi-rigid connections, and the others were rigid connections. Zhang *et al*.

(2012) in [10] investigated Concrete Filled Steel Tubular (CFST) connections by using external diaphragms. Casita *et al*. (2020) [30] analyzed the behaviour of Rectangular Concrete Filled Tubes (RCFT) and Circular Concrete Filled Tubes (CCFT) under axial load. Another investigated study of cold-formed steel connection is added to know the behaviour of steel with a thinness section since RCFT having a thin section profile as outer [31-34].

The RBS connection is one of the most popular ways to weakening the steel beam flange as plastic hinge. Ludovico *et al*. (2013) in [35] investigated that plastic hinge should not occurs near the connection. Their analysis observed that connection with RBS is more effective in reducing the stress concentration at the connection. Casita and Kamandang (2018) in [35] analyzed the behaviour of 3 types of RBS, those are RBS with radius cut, RBS with straight cut, and RBS with tapered cut under monotonic load. Based on the description above, CFT with steel beam connection can provide a good performance, it is expected that can be used for high-rise buildings in strong earthquake areas because of its ductility.

The present study aims to obtain results of numerical modeling on the 2 assemblies of RCFT with and without RBS connections. The main objective include: 1) to make a simple comparison between 2 models on the ductility; 2) to study the effect of the connection on the concentration of stress and strain in different loading scheme; 3) to consider the buckling behaviour of the interior models.

Stress-strain relationship of concrete

Various relations have been studied to examine the strength capacity due to the confinement condition. A vary constitutive model model has been reported in particular for reinforce concrete, such as Kent and Park [36], Rechart *et al*. [37], Popovics [38], Mander *et al*. [39], Chang and Mander [39], etcetera. For the evaluation, a formulation of cyclic characteristics is created by advancing internal variables and incorporating with the constitutive models.

Normalized values of strain, stress and tangent modulus from the expression created of monotonic stress-strain curve in compression is presented in Eqs. (1) - (3).

$$x = \frac{\varepsilon_c}{\varepsilon'_{cc}} \tag{1}$$

$$y = \frac{f'_c}{f'_{cc}} \tag{2}$$

$$n = \frac{E_c \times \varepsilon'_{cc}}{f'_{cc}} \tag{3}$$

$$y = \frac{rx}{r-1+x^r} \tag{4}$$

$$r = \frac{n}{n-1} \tag{5}$$

$$f'_{cc} = f'_c + 4.1 f_1 \tag{6}$$

$$\varepsilon'_{cc} = \varepsilon'_c \left[1 + 5 \times \left(\frac{f'_{cc}}{f'_c - 1}\right)\right] \tag{7}$$

where, x is a variable of normalized strain, y is a variable of normalized stress, n is a variable of normalized modulus, and E_c is initial value of modulus of elasticity. Popovics [40] defined the stress-strain relation equation as popovics's equation. This equation characterize depends on some parameters such as the initial slope and initial modulus of elasticity (E_c) and peak coordinate-strain at the peak point (ε'_{cc}, f'_{cc}), which are modified by Mander *et al*. [39], see Eqs. (4) - (5). The most common for RCFT are developed from those proposed by Rechart *et al*. [41], illustrated in Eqs. (6) - (7), respectively. In which, f'_{cc} is the peak compressive strength of the concrete core; $f'_c$is the peak compressive strength of unconfined concrete, ε'_{cc} is the corresponding strain at the peak compressive strength of the concrete core, and ε'_c is the corresponding strain at the peak compressive strength of unconfined concrete.

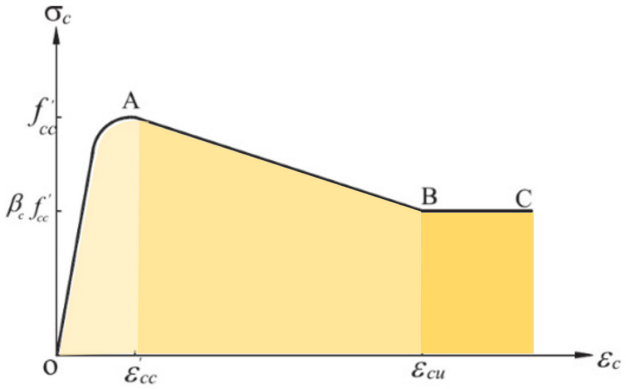

Figure 2 Characteristics of typical stress-strain curve

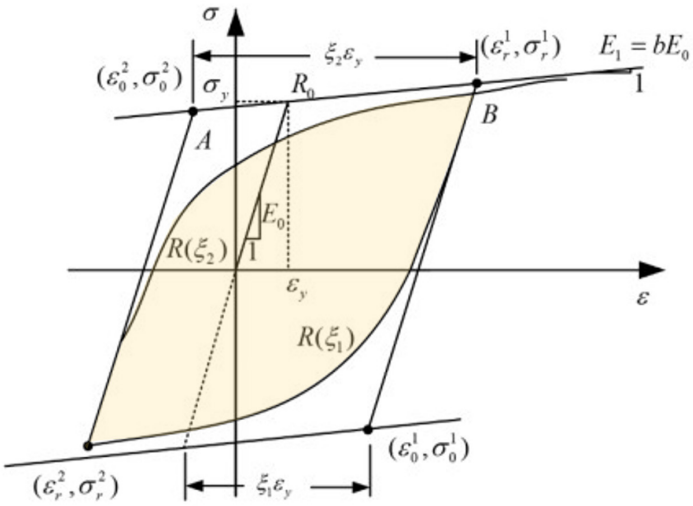

Figure 3 Illustration of stress-strain model of steel under cyclic loading

$$\sigma = b\varepsilon' + \frac{(1-b)\varepsilon'}{(1+\varepsilon'^{R})^{1/R}} \tag{8}$$

$$\varepsilon' = \frac{\varepsilon-\varepsilon_r}{\varepsilon_0-\varepsilon_r} \tag{9}$$

$$\sigma' = \frac{\sigma-\sigma_r}{\sigma_0-\sigma_r} \tag{10}$$

$$E_t = \frac{d\sigma}{d\varepsilon} = \left(\frac{\sigma_0-\sigma_r}{\varepsilon_0-\varepsilon_r}\right)\frac{d\sigma'}{d\varepsilon'} \tag{11}$$

$$R = R_0 \frac{a_1\xi}{a_2-\xi} \tag{12}$$

$$\xi = \left|\frac{(\varepsilon_m-\varepsilon_0)}{\varepsilon_y}\right| \tag{13}$$

Concrete stress-strain relationship

In this study, the steel as the outer are simulated using the widely known as a nonlinear hysteretic which is made by Menegotto and Pinto [42], as modified by Filippou *et al*. [41], to admit isotropic strain-hardening behaviour. Menegotto and Pinto models of the uniaxial hysteretic stress-strain relation [42] are defined as informed in the Eq. (8) and describes the curved transition can be seen in the Eqs. (9) - (10). As the information of the **Figure 3**, where, σ_r and ε_r are the stress and strain relationship at the reversal strain point, σ_0 and ε_0 are in order classified as the stress and strain at the point of intersection of the 2 asymptotes. The strain and stress pairs (ε_r, σ_r) and (ε_0, σ_0) are updated after each strain reversal. Then, the tangent modulus E_t of the stress-strain relation can be expressed by Eq. (11). The curvature factor R is dependent on the absolute strain between the current asymptote intersection point and the previous maximum or minimum strain reversal point, which can be seen in Eq. (12). It is also defined by Menegotto and Pinto [42].

In which, R_0 is the initial variable under monotonic or cyclic loading, a_1 and a_2 are experimentally variables which can reflect the degradation of the curvature within subsequent cycles. ξ is the absolute strain difference between the current asymptote intersection point and the previous maximum or minimum strain reversal point, defined by Eq. (13). In which, ε_m is the minimum or maximum strain at reversal point, ε_0 is the strain value at the current intersection point of the 2 asymptotes, ε_y is the strain at monotonic yield point. Therefore, ξ is evaluated according to the strain reversal.

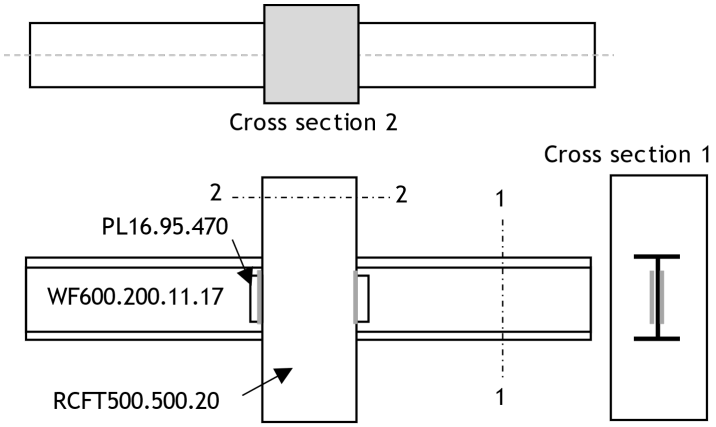

Figure 4 RCFT member without RBS.

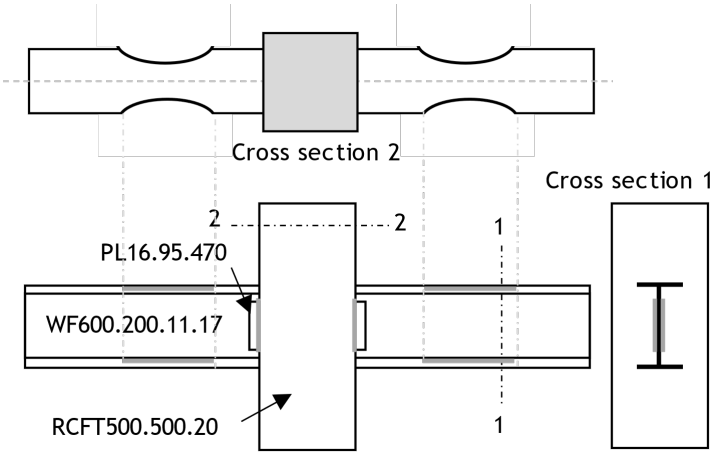

Figure 5 RCFT member with RBS.

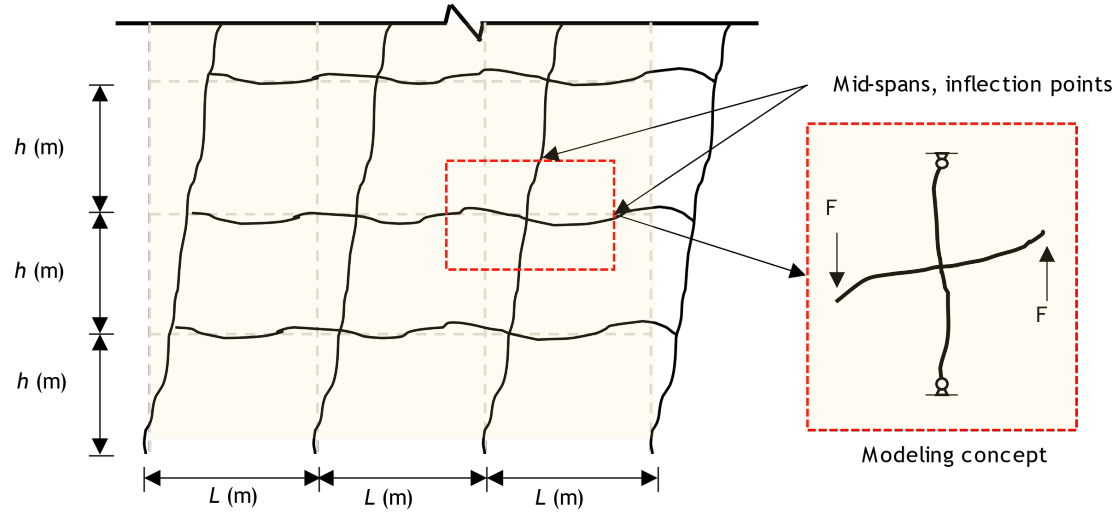

Figure 6 Scheme of loading RCFT structure assembled from interior portal.

Modeling of RCFT member in ABAQUS

Proposed connection details

The analysis from this theoretical simulation included the models of 2-sample of the RCFT, which was built-up in ABAQUS 6.13 - 4 (**Figure 4**) [14,43,44] to figure the behaviour of RCFT on the carrying capacity with and without reduce beam section (RBS) is conducted. The analysis was carried out on the hollow-rectangular cross section using 500×500×20 mm^3 (steel grade 41 according to Indonesian standard) [45-48] with the attached welded plate PL 16.95.470 mm. The length of column is 3,000 mm and the length of the beam is 3,500 mm. The dimensions of the connections are provided in **Figures 4** and **5**. Welded connection is used for these 2 models of connection, with and without RBS.

Finite element model analysis

In the concept of finite element model (FEM), the accuracy of nonlinear both of static and dynamic computational formulas are needed to develop appropriate response factors. The simulated models have to assist directly all inelastic effects from the yielding through strength and stiffness degradation. Further, until the material nearly reaches collapse condition while adequately robust to trail redistribution of inelastic force without concurrence a problem to the point of failure [49]. FEM technique for RCFT structures is now popular due to a widely used RCFT structure. Some unknown parameters are clearly needed to be studied to understand a fully behaviour. Normally, 3-dimensional solid model is used in the numerical analysis. It allows the direct modelling of the composite action between the steel as the outer and concrete components as the filling with different factors. Another aspect of modelling is a coordinate system, imperfection of local and global section, residual stresses and boundary conditions. However, the accuracy of FEM is greatly considered by the parameters input, in particular by selecting a suitable material property and its constitutive model [3,50].

When 3-dimensional solid model is completely made, it allows add another detail parameter to completing the analysis. In this RCFT analysis, the concrete core inside is modeled with solid elements, while the outer steel is modeled with shell elements. To connect the interface between these 2, both material interface is assembled by connector. This connector is simulation the interaction between 2 different material, e.g., steel and concrete components. By using this model analysis, a detail information could possibly be plotted. Most of investigated study by many researchers adopted solid model to analyse the performance capability. Schneider in one of researcher who conducted a comparison study of experimental and analytical program on the behavior of short, CFST columns concentrically loaded in compression to failure [2]. A modelling of mesh of 20 nodes brick element and 8 nodes shell element are used for simulating concrete and steel tube, respectively (**Figure 7**). Another additional study evaluated by Hu *et al*. performing numerical simulations using ABAQUS. The CFST columns model is classified with different cross-sectional shapes subjected to axial compressive loads; circular, square and squared stiffened with confined reinforcing forming an octagonal shape (**Figure 8**) [16].

In term of modelling, ABAQUS library is considered to be used in this evaluation [44]. S4R as well-known as 4-noded doubly curved shell elements is used to model the buckling behavior of the steel outer with added reduced integration. For most application of steel element, the S4R element provides accurate solution since it has 6 degrees of freedom which is positioned per node. The element also allows to transverse shear deformation. In this part, a simulation of thick shell elements is needed. In addition, it is also taking into account for finite strain and sufficient for large strain condition. Coming to the meshing part, C3D8 which is known as 3 dimensional of 8 nodes solid is used to model the concrete inside the steel core. To conduct less computational simulation time with a reasonable result, different mesh sizes have been trialed. As the result, a maximum mesh size within length, width and depth is respectively, 25×25×25 mm^3. For most of the elements in modelling, it can achieve nearly accurate results.

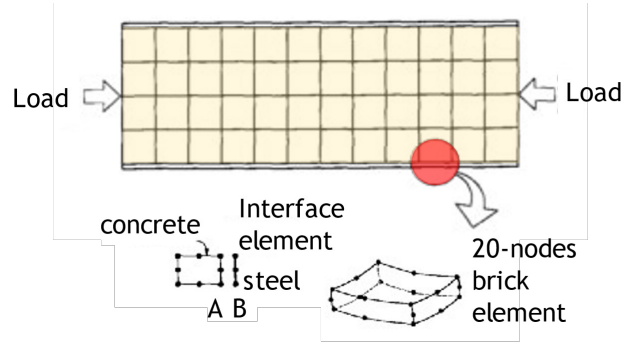

Figure 7 Illustration of FEM by Schneider [2].

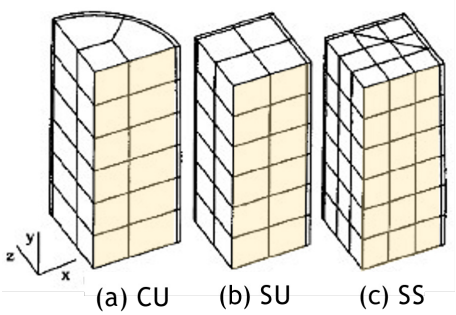

Figure 8 Illustration of FEM by Hu [16].

Boundary conditions and load applications

The concrete inside the steel hollow of RCFT element are left thoroughly unrestrained in all directions. This condition is to allow any possible form of deformation in the RCFT. Another added boundary condition is rigidity. A fictive plate to make the structure rigidi s modelled at both the bottom and top of the model. The condition of rigidity to simulate the platens in an actual testing machine is considered to have a good behaviour. The known fictive plates that are modeled earlier have hinge applied at its reference node. In another hand, the end point of beam is considered to be free and added a cyclic load, which is given oppositely in both sides.

The beam flanges on the RBS model reduced by using circular cutting method. The isotropic - linear kinematic, the rule of hardening with Von Mises yielding criterion is also applied to simulate the plastic deformations on the connection components. This is normally fitted for the metal plasticity simulation under cyclic loading [44]. The interactions between weld-beam-column and plate-beam are defined as tie constraint.

The load was applied on the top of the reference node which is positioned on the beam in the direction of "z" axis. The loading scheme is followed to SAC loading protocol (**Figure 9**). This type of protocol includes more small elastic cycles that occurred before yielding [50]. The cyclic loading wad modelled with a frequent in short term, increasing steadily at a constant rate, introduced through the plate

of a hydraulic press. The simulation of boundary conditions of the connection of the steel and RCFT cross section has been created by using the fictive weld attached to the connection, which means that it was prevented from rotation of this edges. Then, the beam end displacement corresponding to the inter-story drift angle of 0.01 rad was 35 mm.

Modeling of steel and RCFT materials

The material characteristics of the studies were defined by material tests under experimental program. When modelling the steel cross-sections, were used the material characteristics: yield strength *fy* = 250 MPa, ultimate strength *fu* = 410 MPa, elastic modulus E = 200 GPa, Poisson's ratio in elastic state ν = 0.3 were used. Detail information of material is illustrated in **Table 1** followed by the information of stress-strain relationship of steel in **Figures 10 - 12**. Behaviour of material is modelled as elastoplastic with linear hardening according to Park and Paulay [8]. The inside of core of the hollow section was modelled from concrete with a compressive strength, *f'c* = 30 MPa, elastic modulus of concrete E = 26.47 GPa. **Figures 10 - 12** show comparisons of the stress-strain curves under steel and concrete material.

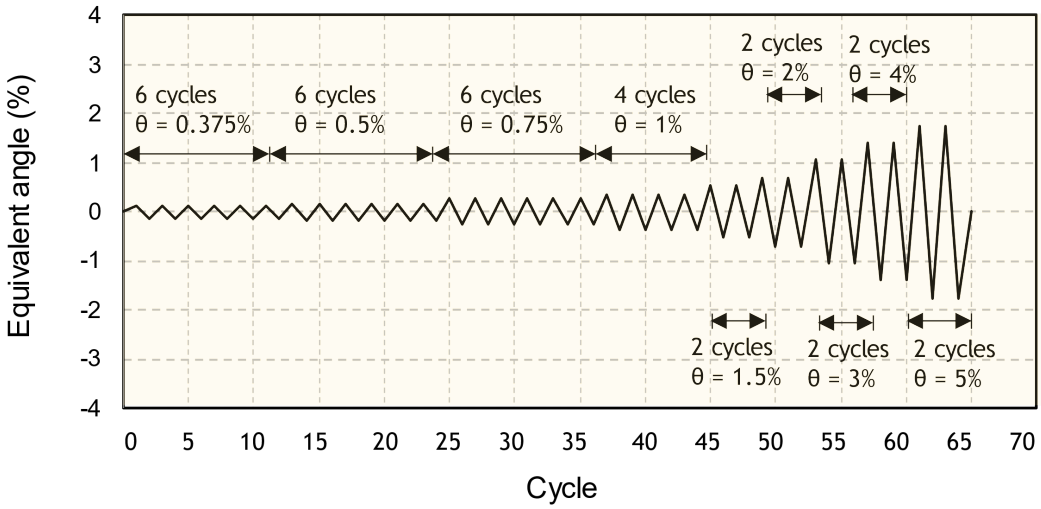

Figure 9 SAC loading protocol applied to the modelling [51].

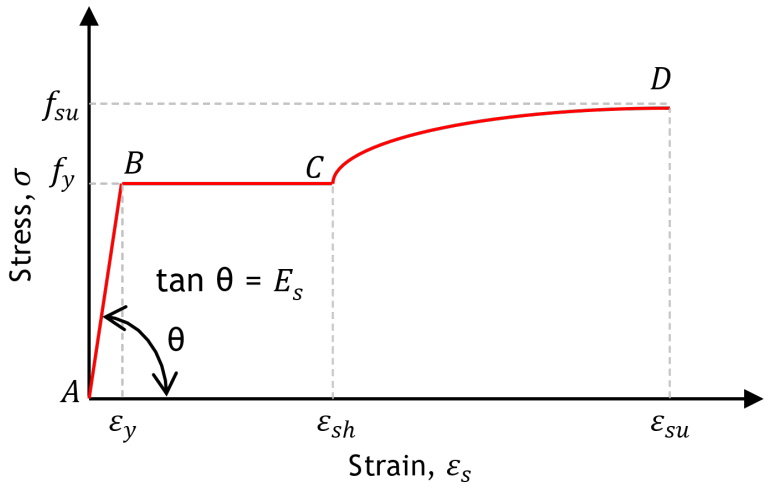

Figure 10 Stress-strain relationship of steel [36].

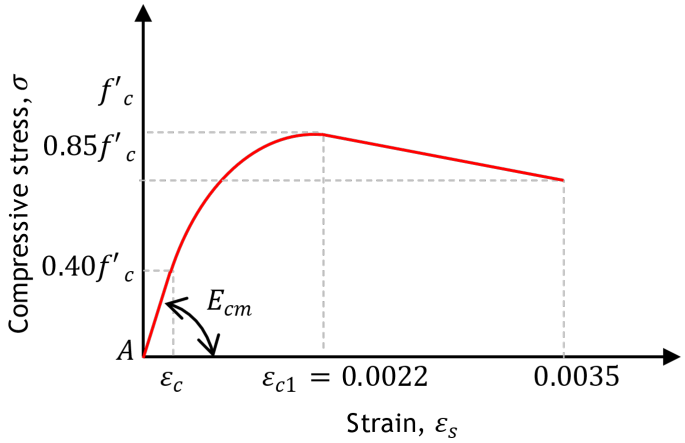

Figure 11 Stress-strain relationship of compressive concrete [36].

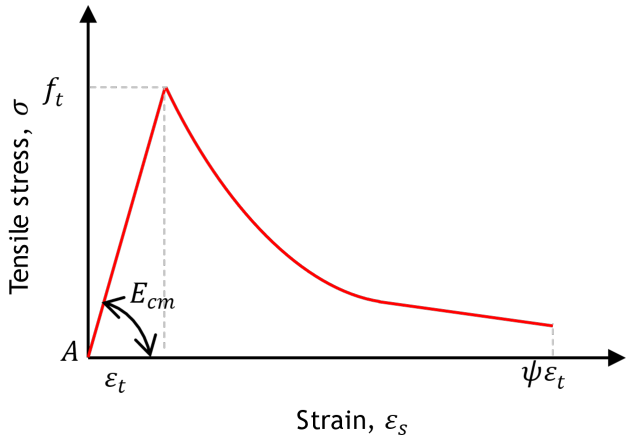

Figure 12 Stress-strain relationship of tensile concrete [36].

Table 1 General specification of the numerical models.

Model	Column and beam size		Length	fy (MPa)	fu (MPa)	Fc' (MPa)
with & without RBS	Column	RCFT 500×500×20	3,000	250	410	30
	Beam	WF 600×200×11×17	3,500			

Table 2 Plasticity of concrete.

Dilatation angle	**38**
Eccentricity	1
$fb_0/f'c$	1.12
K	0.666
Viscosity	0

Results and discussion

The Von Mises stress distribution for 0.05 rad inter story drift angle are shown in **Figure 13**, followed by the stress distribution of S11 (critical force of the first buckling form) in **Figures 14** and **15**. Concentrated stress on RCFT with RBS model occurs in beam and RCFT without RBS occurs in connection. Although RCFT with RBS models, the PZ remained elastic, in RCFT without RBS the PZ had nonlinear behaviour. As it can be seen, the local buckling of beam flange and web has occurred at 5 % rad inter story drift with 32 cycles. As indicated in **Figures 13** - **15**, the brittle cracking my happen on the weld area on RCFT without RBS during cyclic load. Numerically, maximum force of RCFT with RBS lower than RCFT without RBS i.e., 363 MPa - 0.0082 strain and 420 MPa - 0.0125, respectively. The red color implied that the stress nearly to the maximum capacity of the material oppositely with blue color (see the pattern from the color of **Figures 14** and **15**).

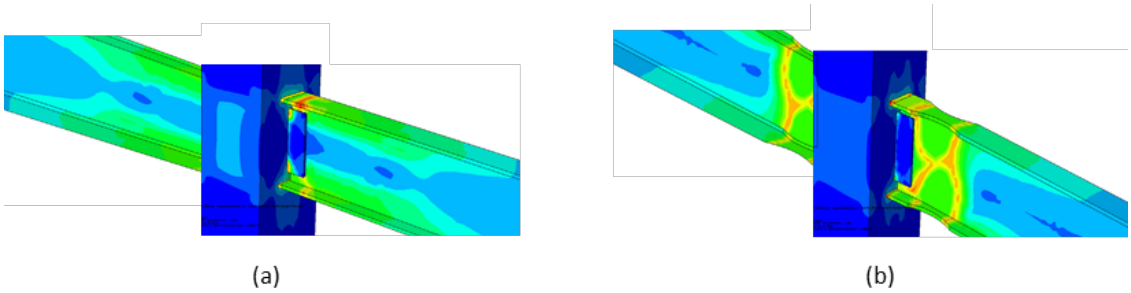

Figure 13 Von mises distribution of RCFT structure; (a) without RBS, (b) with RBS.

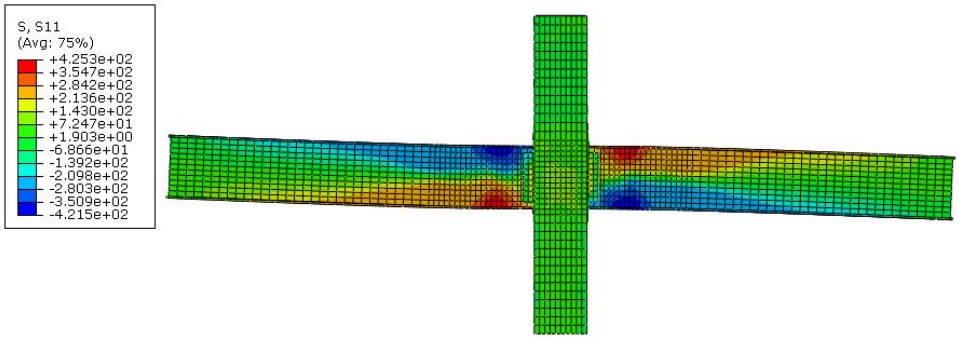

Figure 14 Stress distribution (S11) of structure with RBS.

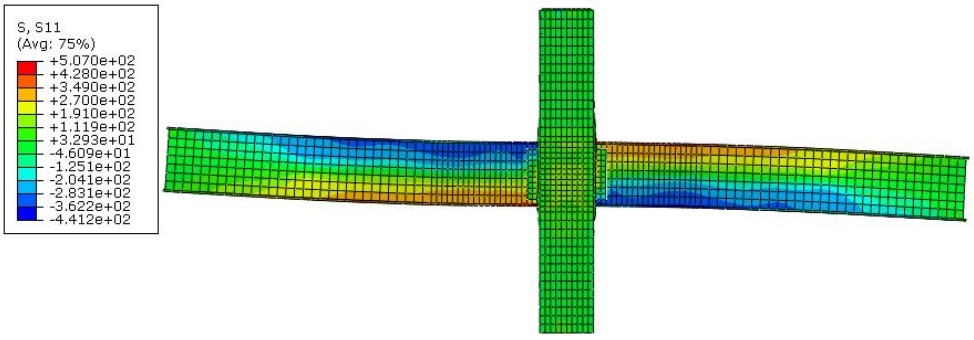

Figure 15 Stress distribution (S11) of structure without RBS.

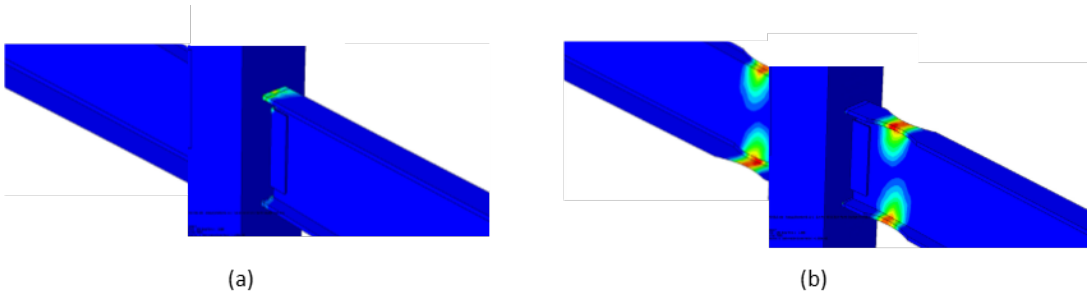

Figure 16 Interactive stress distribution (S11) of structure; (a) without RBS, (b) with RBS.

The plastic equivalent strain in RCFT beam without RBS is not achieved because the fracture is initiated close to the connection. It is also illustrated by the stress distribution of S11 (see **Figures 14** and **15**). It can be seen that concentrated strain of RCFT with RBS models occurs in beam than it occurs in connection. As indicated in **Figure 16**, related to the plastic equivalent strain, the plastic hinge occurs in the connection to the beam. The rupture value is considered to be taken from the plastic equivalent strain that is computed from analysis results.

Table 3 Displacement ductility coefficient.

Model	Yield		Peak		Failure		Ductility
	P_y (kN)	Δ_y (mm)	P_{max} (kN)	Δ_{max} (mm)	P_u (kN)	Δ_u(mm)	μ
RCFT without RBS	54	11	110	33	94	35	3.20
RCFT with RBS	37	20	52	56	44	98	4.90

In contrast to the extensive hysteretic modeling on the behaviour of RCFT with and without RBS under seismic behaviour of interior column connection are illustrated in **Figure 16**. A particular cycles condition is divided based on the loading parameter to know how the structure behave. It can be seen that the hysteretic curves of RCFT with RBS are generally saturated and spindle-squared-shaped, which indicated that the model have better hysteretic behaviour than RCFT without RBS. After the maximum strength achieved, each displacement degrades as cycling proceeds loading, illustrated the wider strain. It is mainly due to increased stress of the RCFT, which will also cause accumulated damage to the in-filled concrete, then cause the stiffness degrades as the vertical displacement increases. However, there is no obvious loading capacity degradation was observed during the given loading under SAC. After that, due to the failure at the beam near to the connection, a sharp decline *P-Δ* appears. The maximum vertical displacement is approximately similar one and another but RCFT with RBS implied saturated hysteric curves than RCFT without RBS.

The required ductility is one of the most concerned characteristics of RCFT with RBS, which is beneficial to evaluate the seismic resistance capability. However, no unified formula is available to determine the ductility of RCFT for both structures. In this model, behaviour of ductility is controlled by the available displacement compared to stress-strain mechanism. Design value of the structural ductility is defined as the ratio if the ultimate limit state displacement d_u to the yield displacement d_y both measured at the center of mass. The ductility coefficient μ of RCFT can be defined as Δ_u / Δ_y where Δ_u is the lateral displacement corresponding to P_u which is 85 % of the ultimate lateral load P_{max}. Δ_y is the lateral displacement when the cross section of RCFT is in yield range. The yield displacement can be defined as the displacement of the intersection point of 2 lines when the initial elastic tangent of the envelop curve and the flat tangent of the ultimate point on the envelop curve.

From **Figure 17**, envelope curves of stress and strain, the force and displacement of yield point, peak point and failure point can be calculated, then the ductility coefficient of those 2 models are obtained (**Table 3**).

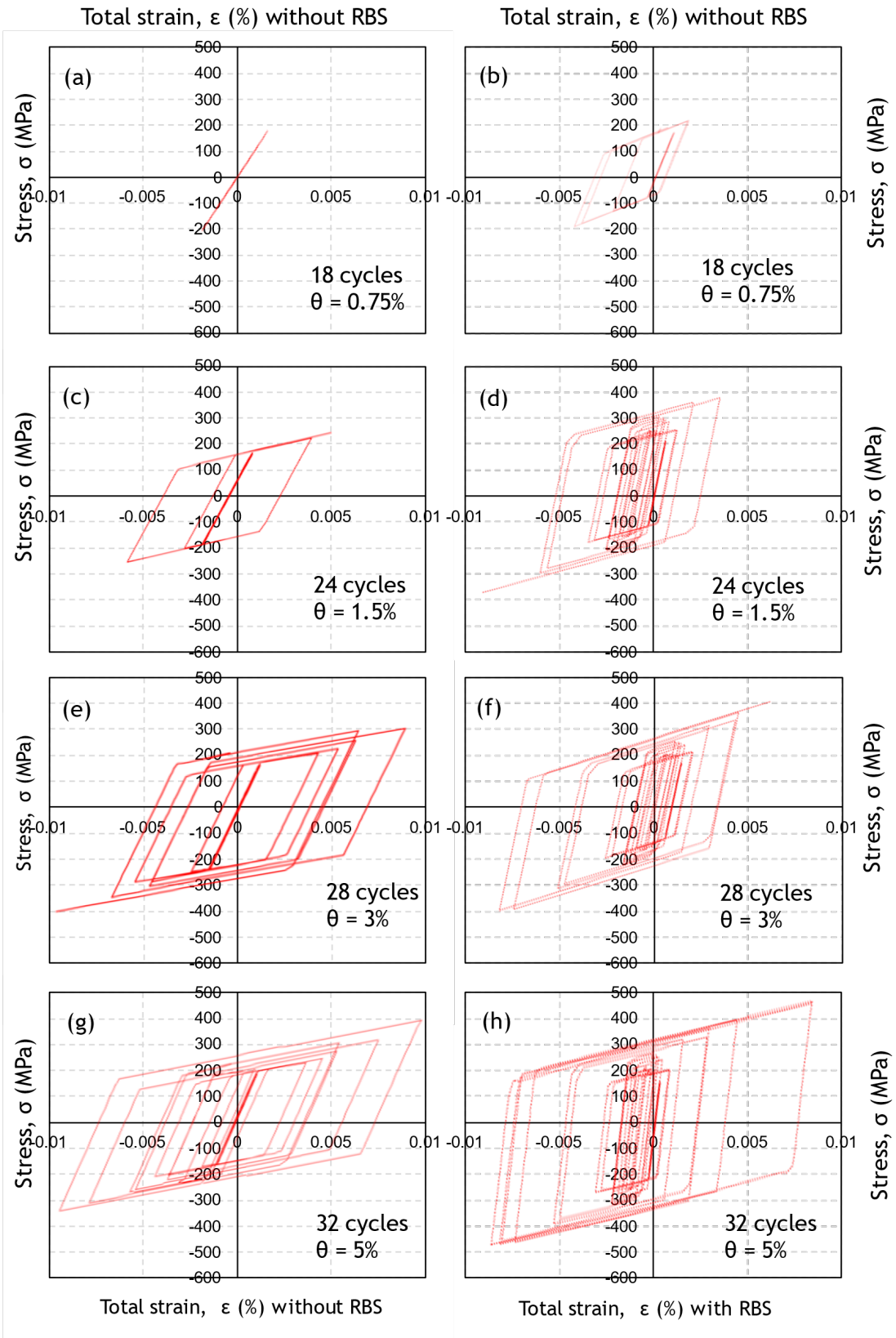

Figure 17 Change in the stress-strain hysteresis loop as the number of increased cycles with and without RBS at a total strain; (a) ± 0.75 % without RBS, (b) ± 0.75 % with RBS, (c) ± 1.5 % without RBS, (d) ± 1.5 % with RBS, (e) ± 3 % without RBS 28 - cycle, (f) ± 3 % with RBS 28 - cycle, (g) ± 5 % without RBS 32 - cycle, (h) ± 5 % with RBS32-cycle.

The total stress and the total strain were measured at the column face and the total beam rotation under the displacement criteria by the distance of the column face. As it can be observed, all models have suitable hysteric behaviour. Consequently, this connection satisfies the criteria of AISC seismic provisions (2005) for special moment frame system. For the future work, the evaluation will be compared to the experimental program concentrate to the same loading parameter.

Conclusions

Based on the results of this theoretical analysis from modelling by ABAQUS as general conclusion of the research were provided:

1) In the RCFT with RBS, plastic deformation take place in the beam significantly.

2) RCFT with RBS implying better ductility than RCFT without RBS in terms of the cyclic resistance. By usin,g RBS it also relocates plastic hinges away from the column face.

3) Theoretically, RCFT analysis is one part of the research oriented to determine the impact of ductility and loss stability of RCFT elements according to their resistance. Based on both models shown in hysteretic curves, RCFT with and without RBS significantly affect the stability. This one, because the concrete core inside the column increases the resistance from the loss of local and global stability.

References

[1] J Zheng and J Wang. Concrete-filled steel tube arch bridges in China. *Engineering* 2018; 4, 143-55.

[2] SP Schneider and YM Alostaz. Experimental behavior of connections to concrete-filled steel tubes. *J. Constructional Steel Res.* 1998; 45, 321-52.

[3] H Lin-Hai, Y Guo-Huang and Z Tao. Performance of concrete-filled thin-walled steel tubes under pure torsion. *Thin Walled Struct.* 2007; **45**, 24-36.

[4] H Lin-Hai, H Huang and Z Xiao-Ling. Analytical behaviour of concrete-filled double skin steel tubular (CFDST) beam-columns under cyclic loading. *Thin Walled Struct.* 2009; **47**, 668-80.

[5] F Abed, MA Hamaydeh and S Abdalla. Experimental and numerical investigations of the compressive behavior of concrete filled steel tubes (CFSTs). *J. Constructional Steel Res.* 2013; **80** 429-39.

[6] H Lin-Hai. Flexural behaviour of concrete-filled steel tubes. *J. Constructional Steel Res.* 2004; **60**, 313-37.

[7] R Kanishchev and V Kvocak. Stability and carrying capacity of the steel tubes. *Procedia Eng.* 2017; **190**, 447-51.

[8] E Jahanbakhti, N Fanaie and A Rezaeian. Experimental investigation of panel zone in rigid beam to box column connection. *J. Constructional Steel Res.* 2017; **137**, 180-91.

[9] Y Du, Z Chen, JYR Liew and X Ming-Xiang. Rectangular concrete-filled steel tubular beam-columns using high-strength steel: Experiments and design. *J. Constructional Steel Res.* 2017; **131**, 1-18.

[10] Y Zhang and D Li. Development and testing of precast concrete-filled square steel tube column-to-RC beam connections under cyclic loading. *Construct. Build. Mater.* 2021; **280**, 122540.

[11] C Ding, Y Bai, K Yang and J Zhang. Cyclic behaviour of prefabricated connections for steel beam to concrete filled steel tube column. *J. Constructional Steel Res.* 2021; **176**, 106422.

[12] MMA Khanouki, NHR Sulong, M Shariati and MM Tahir. Investigation of through beam connection to concrete filled circular steel tube (CFCST) column. *J. Constructional Steel Res.* 2016; **121**, 144-62.

[13] TM Tran, B Matuszkiewicz and MNS Hadi. Response of substandard reinforcing details T connections upgraded with concrete covers and CFRP. *In*: Proceedings of the 4th Asia-Pacific Conference on FRP in Structures, Canada. 2013, p.1-10.

[14] P Doung and E Sasaki. Load-deformation characteristics and performance of internal diaphragm connections to box columns. *Thin Walled Struct.* 2019; **143**, 106221.

[15] JM Flor, RH Fakury, RB Caldas, FC Rodrigues and AHM Araújo. Experimental study on the flexural behavior of large-scale rectangular concrete-filled steel tubular beams. *Rev. IBRACON Estruturas e Materiais* 2017; **10**, 895-905.

[16] F Hu, G Shi, Y Bai and Y Shi. Seismic performance of prefabricated steel beam-to-column connections. *J. Constructional Steel Res.* 2014; **102**, 204-16.

[17] W Jing-Feng, H Lin-Hai and B Uy. Behaviour of flush end plate joints to concrete-filled steel tubular columns. *J. Constructional Steel Res.* 2009; **65**, 925-39.

[18] H Hsuan-Teh, H Chiung-Shiann, W Ming-Hsien and W Yih-Min. Nonlinear analysis of axially

loaded concrete-filled tube columns with confinement effect. *J. Struct. Eng.* 2003; **129**, 1322-9.
[19] AK Patidar. Behaviour of concrete filled rectangular steel tube column. *IOSR J. Mech. Civ. Eng.* 2012; **4**, 46-52.
[20] D Zhang, S Gao and J Gong. Seismic behaviour of steel beam to circular CFST column assemblies with external diaphragms. *J. Constructional Steel Res.* 2012; **76**, 155-66.
[21] MA Bastian, A Tambusay, I Komara, W Sutrisno, D Irawan and P Suprobo. Enhancing the ductility of a reinforced concrete beam using engineered cementitious composite. *IOP Conf. Series: Earth Environ. Sci.* 2020; **506**, 012044.
[22] I Komara, A Tambusay, W Sutrisno, P Suprobo and D Iranata. The investigation study of improving durability performance of marine infrastructure by using the engineered cementitious composite. *In*: Proceedings of the 14th International Student Conference on Advanced Science and Technology, Kumamoto, Japan. 2019, p. 8-12.
[23] WN Oktaviani, A Tambusay, I Komara, W Sutrisno, F Faimun and P Suprobo. Flexural behaviour of a reinforced concrete beam blended with fly ash as supplementary material. *IOP Conf. Series: Earth Environ. Sci.* 2020; **506**, 012042.
[24] I Komara, P Suprobo, D Iranata, A Tambusay and W Sutrisno. Experimental investigations on the durability performance of normal concrete and engineered cementitious composite. *IOP Conf. Series: Mater. Sci. Eng.* 2020; **930**, 012056.
[25] I Komara, A Tambusay, W Sutrisno and P Suprobo. Engineered cementitious composite as an innovative durable material: A review. *ARPN J. Eng. Appl. Sci.* 2019; **14**, 822-33.
[26] M Mooy, A Tambusay, I Komara, W Sutrisno, Faimun and P Suprobo. Evaluation of shear-critical reinforced concrete beam blended with fly ash. *IOP Conf. Series: Earth Environ. Sci.* 2020; **506**, 012041.
[27] E Susanti, H Istiono, I Komara, D Pertiwi, Y Septiarsilia and FK Syahputra. Effect of fly ash to water-cement ratio on the characterization of the concrete strength. *IOP Conf. Series: Mater. Sci. Eng.* 2021; **1010**, 012035.
[28] W Xua, H Lin-Hai and Z Tao. Flexural behaviour of curved concrete filled steel tubular trusses. *J. Constructional Steel Res.* 2014; **93**, 119-34.
[29] C Sing-Ping, L Seng-Tjhen and D Chao-Wei. Moment resistance of steel i-beam to CFT column connections. *J. Struct. Eng.* 2001; **127**, 1164-72.
[30] CB Casita, IPE Sarassantika and R Sulaksitaningrum. Behaviour of rectangular concrete filled tubes and circular concrete filled tubes under axial load. *J. Appl. Sci. Manag. Eng.* 2020; **1**, 14-20.
[31] I Komara, K Taskin, E Wahyuni and P Suprobo. Experiment on cold-formed steel c-section joint with screw ond adhesive material. *Int. J. Sci. Tech.* 2017; **3**, 51-63.
[32] I Komara, E Wahyuni and P Suprobo. A study on cold-formed steel frame connection : A review. *IPTEK J. Tech. Sci.* 2017; **28**, 83-9.
[33] I Komara, E Wahyuni, P Suprobo and K Taskin. Assessing the tensile capacity of cold-formed steel connections using self-drilling screws and adhesive materials. *Int. J. Adv. Sci. Eng. Inform. Tech.* 2018; **8**, 398-404.
[34] I Komara, E Wahyuni, P Suprobo and K Taskin. Micro-structural characterization of the bond strength capacity of adhesive material in the alternative of cold-formed steel frame system. *IOP Conf. Series: Mater. Sci. Eng.* 2019; **462**, 012004.
[35] MD Ludovico, M Polese, MG Aragona, A Prota and G Manfredi. A proposal for plastic hinges modification factors for damaged RC columns. *Eng. Struct.* 2013; **51**, 99-112.
[36] RG Selby and FJ Vecchio. A constitutive model for analysis of reinforced concrete solids. *Can. J. Civ. Eng.* 1997; **24**, 460-70.
[37] FE Richart. *Tests of the effect of brackets in reinforced concrete rigid frames*. Vol 1. National Bureau of Standards, Maryland, 1928, p. 189.
[38] R Kanishchev and V Kvocak. Local buckling of axially compressed rectangular concrete-filled steel tubes. *MATEC Web Conferences* 2016; **73**, 04017.
[39] GA Chang. *Seismic energy based fatigue damage analysis of bridge columns*. University Microfilms International, Michigan, 1993.
[40] G Shi, H Fan, Y Bai, F Yuan, YJ Shi and YQ Wang. Improved measure of beam-to-column joint rotation in steel frames. *J. Constructional Steel Res.* 2012; **70**, 298-307.
[41] M Midorikawa, T Ishihara, T Azuhata, T Asari, H Hori and T Kusakari. Seismic behavior of steel rocking frames by three-dimensional shaking table tests. *Response* 2010; **10**, 1085-90.
[42] M Menegotto and PE Pinto. Method of analysis for cyclically loaded R.C. plane frames including changes in geometry and non-elastic behavior of elements under combined normal force and

bending. ETH Library, Zürich, Switzerland, 1973, p. 15-22.
[43] Portland State University. *Abaqus/CAE material nonlinearity tutorial*. Portland State University, Portland, 2011.
[44] Portland State University. *Abaqus CAE*. Portland State University, Portland, 2010.
[45] Badan Standardisasi Indonesia. *Tata cara perencanaan ketahanan gempa untuk struktur bangunan gedung dan non gedung.* Badan Standardisasi Nasional, Indonesian, 2003.
[46] Standar Nasional Indonesia. *Beban minimum untuk perancangan bangunan gedung dan struktur lain*. Badan Standardisasi Nasional, Indonesian, 2018.
[47] Rancangan Standar Nasional Indonesia 2. *Persyaratan beton struktural untuk bangunan gedung dan penjelasan (ACI 318M-14 dan ACI 318RM-14, MOD)*. Badan Standardisasi Nasional, Indonesian, 2019.
[48] Standar Nasional Indonesia. *Persyaratan beton struktural untuk bangunan gedung*. Badan Standardisasi Nasional, Indonesian, 2013.
[49] SL Jones, GT Fry and MD Engelhardt. Experimental evaluation of cyclically loaded reduced beam section moment connections. *J. Struct. Eng.* 2002; **128**, 441-51.
[50] P Kral, P Hradil, J Kala, F Hokes and M Husek. Identification of the Parameters of a concrete damage material model. *Proc. Eng.* 2017; **172**, 578-85.
[51] Y Jiao, S Kishiki and S Yamada. Loading protocols employed in evaluation of seismic behavior of steels beams in weak-beam moment frames. *In*: Proceedings of the 15th World Conference on Earthquake Engineering 2012, Lisbon, Portugal. 2012.